

Development of barium@alginate adsorbents for sulfate removal in lithium refining

Lisa Xu, Kaifei Chen, George Q. Chen, Sandra E. Kentish, Gang (Kevin) Li (✉)

Department of Chemical Engineering, The University of Melbourne, Parkville, VIC 3010, Australia

© Higher Education Press 2020

Abstract The demand for lithium has been steadily growing in recent years due to the boom of electric cars. High purity lithium is commonly used in the manufacture of battery grade lithium electrolyte. Sulfate residuals originating from acid leaching of lithium ores must be limited to below $20 \text{ mg}\cdot\text{L}^{-1}$ during refining. There are methods to remove sulfate such as membrane processing and chemical precipitation using barium salts. However, membrane separation is unable to achieve the required purity while chemical precipitation often causes secondary contamination with barium and requires extra filtration processes that lead to increased processing costs. In this study, we developed a polymeric matrix entrapped with barium ions as a novel adsorbent to selectively adsorb sulfate in aqueous solutions. The adsorbent was prepared by dropwise injection method where alginate droplets were crosslinked with barium to form hydrogel microcapsules. In a typical scenario, the microcapsules had a diameter of 3 mm and contained 5 wt-% alginate. The microcapsules could successfully reduce sulfate concentration in a solution from 100 to $16 \text{ mg}\cdot\text{L}^{-1}$, exceeding the removal target. However, the microcapsules were mechanically unstable in the presence of an excess amount of sulfate. Hence, calcium ions were added as a secondary cross-linking agent to improve the integrity of the microcapsules. The two-step Ca/Ba@alginate microcapsules showed an exceptional adsorption performance, reducing the sulfate concentration to as low as $0.02 \text{ mg}\cdot\text{L}^{-1}$. Since the sulfate selective microcapsules can be easily removed from the aqueous system and do not result in secondary barium contamination, these Ca/Ba@alginate adsorbents will find applications in ultra-refining of lithium in industry.

Keywords barium@alginate, microcapsules, dropwise injection, sulfate removal, lithium

1 Introduction

The demand for lithium-ion batteries has grown with the popularity of electric cars and mobile devices [1]. The cathode of lithium-ion batteries uses lithium metal oxide, which is made from lithium compounds extracted from lithium deposits, such as high purity lithium hydroxide or lithium carbonate. Apart from brines, rock deposits are the most common form of lithium particularly in Australia, Canada, and China [2]. The conventional way to extract lithium from pegmatite containing spodumene [3] includes calcination at above $1050 \text{ }^\circ\text{C}$ to loosen the lattice to form β -spodumene, followed by leaching with concentrated sulfuric acid [4] to extract the lithium. The leaching process results in a lithium sulfate concentrate. This is then purified and reacted with sodium carbonate or calcium hydroxide to produce lithium carbonate [5] or lithium hydroxide [6]. A sulfate content below 0.01 wt-% must be obtained within the solid product, which corresponds to a sulfate concentration of less than $20 \text{ mg}\cdot\text{L}^{-1}$ in a saturated solution of 10.9 wt-% lithium hydroxide at $20 \text{ }^\circ\text{C}$ for battery grade lithium production [7].

There are a few existing methods, including membrane separation and chemical precipitation [8] for such lithium solution purification. Membrane separation uses charged membranes and Donnan exclusion theory to separate the differently charged ions [9], but is often prone to fouling and is incapable of producing ultra-high purity products [10]. Chemical precipitation normally uses barium ions to precipitate sulfate ions to form insoluble barium sulfate, which has a solubility equilibrium constant (K_{sp}) of 1.08×10^{-10} [11] with the following reaction [12].



This reaction makes chemical precipitation very selective and relatively inexpensive given the raw material used. However, barium sulfate can form very fine particles that often need to be separated using microfiltration [13]. Furthermore, the quantity of barium ions added needs to be

stoichiometric, or the excess barium ions require an extra step to be removed, which substantially increases the operation complexity and operating costs.

This research focuses on the development of a polymeric matrix material with entrapped barium to selectively adsorb sulfate. Barium ions are encapsulated within microcapsules to resolve the aforementioned challenges in the conventional precipitation process while effectively removing the sulfate ions from the solution. Alginate was selected as the ligand material for the preparation of the polymeric microcapsules, due to its known ability to gel in the presence of multivalent cations such as Ba^{2+} and Ca^{2+} . Conversely, the carboxyl groups on the alginate, with a single negative charge do not induce gelation with monovalent cations such as lithium [14]. Other advantages of such polymers include easy accessibility, low cost, biodegradability, and non-toxicity [15,16].

In this study, we aim to develop a novel barium@alginate adsorbent for sulfate removal in lithium refining. The research goal is to reduce the sulfate concentration to less than $20 \text{ mg} \cdot \text{L}^{-1}$ in the solution. A range of microcapsules prepared under different reaction conditions were studied in terms of Ba^{2+} loading, morphology, integrity, effectiveness and kinetics of sulfate removal. The findings of this work will contribute to future development of more efficient and environmentally friendly separation processes for lithium refinery.

2 Experimental

2.1 Chemicals

$\text{Ba}(\text{OH})_2 \cdot 8\text{H}_2\text{O}$ (98.0 wt-%), $\text{Li}_2\text{SO}_4 \cdot \text{H}_2\text{O}$ (99.0 wt-%) and alginate sodium salt were purchased from Sigma-

Aldrich. $\text{CaCl}_2 \cdot 2\text{H}_2\text{O}$ (99.0 wt-%) and $\text{BaCl}_2 \cdot 2\text{H}_2\text{O}$ (99.0 wt-%) were purchased from Chem-supply.

2.2 Synthesis of microcapsules

Three methods were developed to produce the barium@alginate microcapsules. The first method uses pure barium hydroxide as the gelation reagent to produce the Ba@alginate microcapsules as shown in Fig. 1(a). In a typical procedure, 0.5 g of alginic acid sodium salt was dissolved into 10 mL of deionised water; next, 0.5 g of $\text{Ba}(\text{OH})_2 \cdot 8\text{H}_2\text{O}$ was dissolved in 50 mL of deionised water; then, the alginate was added to the barium hydroxide solution at room temperature drop by drop, using a syringe with gauge of $21\text{G} \times 1.5''$ from a height of at least 15 cm, to allow for spherical gel beads to form. The alginate microcapsules were left to stand in the barium solution for 60 min and were then collected, rinsed with deionised water and dried by patting with a paper towel. The microencapsulation process was repeated with 2, 3, 4, 5, and 6 wt-% alginate solutions to study the impact of alginate concentration.

The second method attempted to produce Ca/Ba@alginate microcapsules in two gelation steps as shown in Fig. 1(b). The alginate solution was injected dropwise into 50 mL of a $0.1 \text{ mol} \cdot \text{L}^{-1}$ of CaCl_2 solution, and crosslinked for 5 min to form calcium firmed microcapsules. The microcapsules were transferred onto a sieve and rinsed with deionised water immediately to terminate the cross-linking process. Next, the microcapsules were immersed into 50 mL of $0.1 \text{ mol} \cdot \text{L}^{-1}$ barium chloride solution and further crosslinked with Ba^{2+} for an hour. Finally, the microcapsules were collected, rinsed with deionised water and dried with a paper towel.

In the third method two firming agents, namely Ca^{2+} and

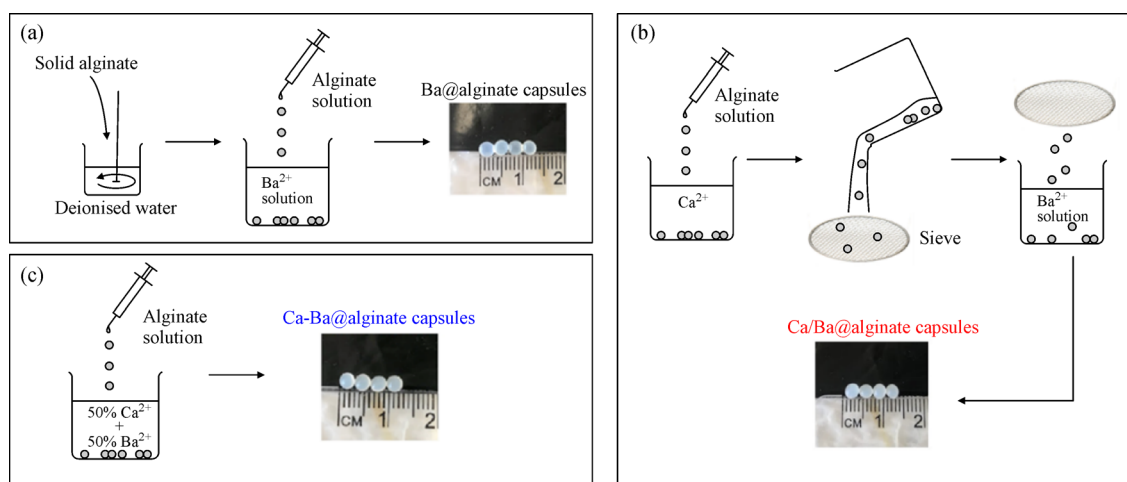


Fig. 1 Methods for preparing Ba@alginate microcapsules: (a) Method 1, pure barium hydroxide Ba@alginate microcapsules; (b) Method 2, two-step Ca/Ba@alginate microcapsules, where the polymerisation reaction first took place by using calcium as the firming agent, followed by barium; (c) Method 3, one step dual-ion Ca-Ba@alginate microcapsules, where both calcium and barium ions were used for the polymerisation reaction at the same time.

Ba²⁺, were involved at the same time for the preparation of the one step dual-ion Ca-Ba@alginate microcapsules as shown in Fig. 1(c). First, 50 mL of 0.1 mol·L⁻¹ barium chloride solution and 50 mL of 0.1 mol·L⁻¹ calcium chloride solution were well mixed at room temperature. The alginate solution was injected dropwise into the mixed-cation solution using a syringe with gauge of 21G × 1.5", and crosslinked for an hour. The microcapsules were collected, rinsed and dried as before.

2.3 Characterisation of microcapsules

The shapes of the microcapsules were visually observed. Their sizes were measured using a ruler and the average of the measurements for four microcapsules was reported.

A physical strength test was carried out by using an electronic balance. Increasing pressure was applied to the microcapsule against the balance under a glass plate until it ruptured, while the force was recorded. This process was repeated three times for the same type of microcapsules and the average value was calculated.

The structural integrity of the Ba@alginate microcapsules was tested with excess sulfate. Typically, ten microcapsules from the same batch were soaked in 10 mL of 800 mg·L⁻¹ lithium sulfate solution for 4 h, and the broken microcapsules were visually observed. The integrity was calculated as the ratio of the number of microcapsules that survived to that of microcapsules tested.

2.4 Effectiveness of sulfate removal

The effectiveness of Ba@alginate microcapsules for sulfate removal was tested as follows. In a typical scenario, 0.2 g of microcapsules were immersed in 10 mL of 100 mg·L⁻¹ lithium sulfate solution in an enclosed container that was left to stand for 4 h. The sulfate concentration in the solution after adsorption was tested to calculate sulfate removal efficiency using Eq. (2).

$$\text{sulfate removal efficiency} = \frac{(C_0 - C_e)}{C_0} \times 100, \quad (2)$$

where C_0 and C_e (mg·L⁻¹) is the concentration of sulfate in the solution before and after adsorption, respectively.

2.5 Kinetics of sulfate adsorption

The kinetics of sulfate removal by adsorption was determined by submerging 0.2 g of microcapsules in 10 mL of 100 mg·L⁻¹ lithium sulfate solution in an enclosed container for periods of 5, 10, 20, 30 min, and 1, 2, 3, 4, 5 h. The concentration of the solution after adsorption was tested. The amount of sulfate (Q) removed at time t , was calculated by the following equation:

$$Q = \frac{(C_0 - C_t)V}{m}, \quad (3)$$

where C_0 (mg·L⁻¹) is the initial concentration of the sulfate solution, C_t (mg·L⁻¹) is the sulfate concentration at time t (s), m (g) is the mass of the microcapsules submerged, and V (L) is the volume of the sulfate solution.

2.6 Analytical methods

The sulfate solution after adsorption was filtered with 0.45 μm membrane filters, and tested with ion chromatography (Thermo Scientific Dionex ICS 1100 and Autosampler AS40). Scanning electron microscopy (SEM, Quanta) with an energy dispersive X-ray spectrometer (EDS) was conducted before and after sulfate adsorption on the microcapsules to observe the morphology as well as the distribution of the adsorption sites inside the microcapsules. The SEM samples were prepared by drying the microcapsules in a vacuum oven at 80 °C overnight, cutting into half, and mounting with carbon tape. An accelerating voltage of 10.00 kV was used by the SEM/EDS. with results smoothed with a Savitzky-Golay filter by a 2-point quadratic polynomial and 10 points of window.

3 Results and discussion

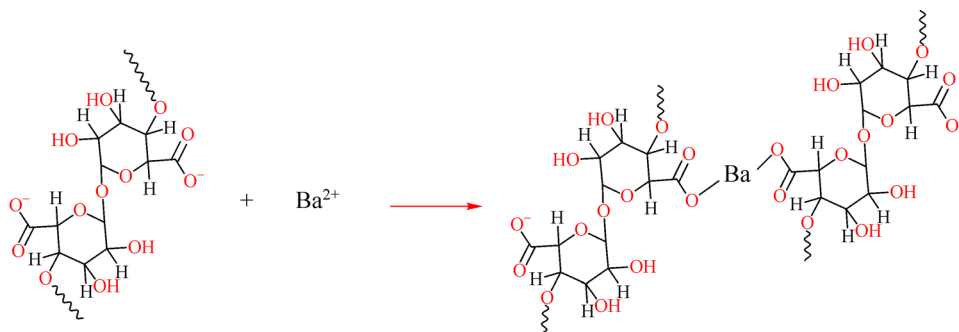
Alginate can undergo gelation reactions with multivalent cations such as Ca²⁺ and Ba²⁺, forming ionic bonds with the carboxyl groups present [14], as shown in Scheme 1.

Calcium is selected for the reinforcement of the Ba@alginate microcapsules, since calcium ions are able to crosslink with alginate to form a stronger calcium@alginate hydrogel, which is non-toxic, low in cost and is widely used [17]. These properties greatly increase the versatility of the microcapsules.

3.1 Morphology and optimisation

The Ba@alginate microcapsules prepared with different weight percentages of alginate are shown in Fig. 2. The optimum concentration of alginate was selected by balancing the shape of the product microcapsules and the amount of alginate used. More uniform spheres enable adsorption to take place more evenly and offer better packing inside the adsorption column. Moreover, a higher ratio of alginate results in more carboxyl functional groups (R-COOH) available, leading to higher loading of barium and thus greater sulfate adsorption capacity, which is a desirable characteristic.

The 2 wt-% Ba@alginate was not able to form spherical microcapsules. The low viscosity of the alginate solution meant that the droplets were unable to keep their sphericity



Scheme 1 Barium ion crosslinks with carboxyl functional groups.

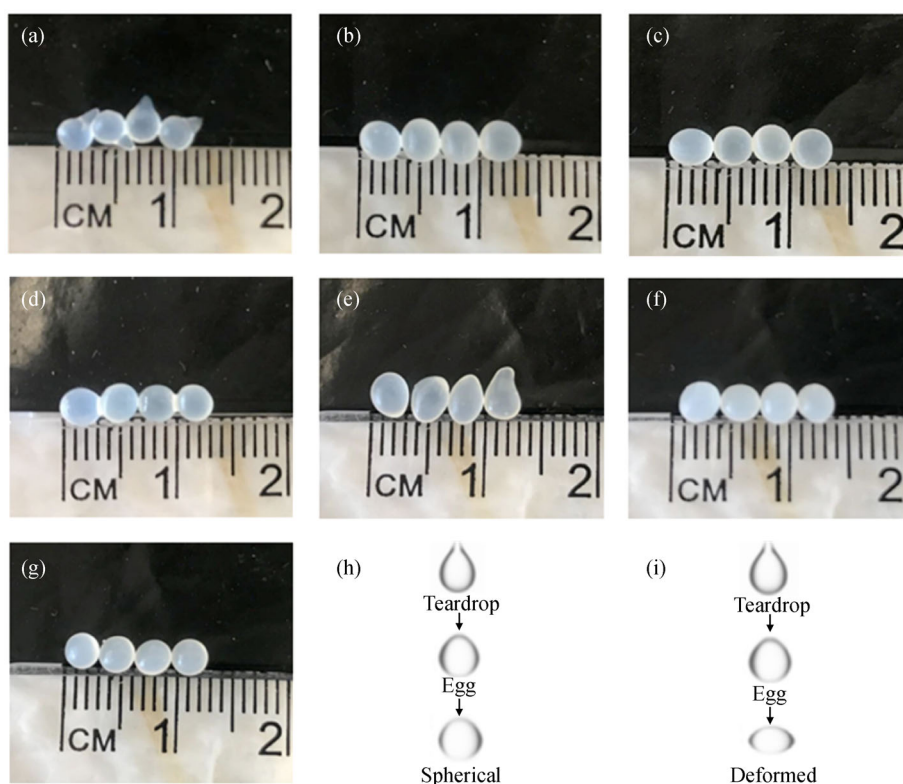


Fig. 2 Optical images of Ba@alginate microcapsules prepared using three methods at different alginate concentrations: (a–e) Ba@alginate microcapsules produced from 2, 3, 4, 5, and 6 wt-% alginate, respectively; (f) Ca/Ba@alginate from 5 wt-% alginate; (g) Ca-Ba@alginate from 5 wt-% alginate. Illustrations of the alginate solution dropwise injection process (h) under the desirable range of viscosity and (i) under high viscosity.

from the minimum height (at least 15 cm) [18] as they hit the surface of the solution. Instead, the droplets flattened as they hit the liquid surface. In order to avoid this deformation, we decreased the dropping height to as low as 1 cm above the liquid surface. However, at these shorter distances, teardrop shaped microcapsules were formed as shown in Fig. 2(a), which is not suitable for packed columns.

Similarly, we were unable to obtain spherical microcapsules using 6 wt-% alginate (Fig. 2(e)). The alginate

liquid transforms from a teardrop shape to an egg shape, and then a spherical shape (Fig. 2(h)). However, due to the high viscosity, the surface tension force is reduced, which fails to compete against the air drag force pushing up against the bottom of the droplet [19]. Hence the droplet was deformed to an oval shape as illustrated in Fig. 2(i).

As shown in Figs. 2(b)–2(d), 3, 4 and 5 wt-% alginates are able to form spherical microcapsules. The sizes of the microcapsules are very similar, with diameters around 3 mm. Five wt-% alginate was selected for the synthesis of

the microcapsules, as it provides a greater loading of barium in the microcapsules and thus a more compact packing in a column.

Since the preparation step for the alginate solution was the same for all production methods of Ba@alginate microcapsules, 5 wt-% alginate was also selected for synthesis of Ca/Ba@alginate and Ca-Ba@alginate microcapsules. The optical images of the microcapsules prepared as Ca-Ba@alginate are shown in Figs. 2(f) and 2(g), from which we can see the microcapsules are of high sphericity with diameters also around 3 mm, in a semi-transparent white colour similar to Ba@alginate microcapsules.

3.2 Structure integrity of the microcapsules

As shown in Fig. 3(a) Inset, it was found that the microcapsules tended to rupture into flakes in excessively high concentration of lithium sulfate solutions (i.e., $800 \text{ mg} \cdot \text{L}^{-1}$). Figure 3(a) illustrates a positive relationship between the mass fraction of alginate and the microcapsule integrity. As the alginate percentage increases, more microcapsules survive in the solution within a sulfate concentration of $800 \text{ mg} \cdot \text{L}^{-1}$. It is well known that sulfate reacts with barium cations to form insoluble precipitates [12]. The excessive sulfate depletes the Ba^{2+} from the Ba@alginate crosslinks, disrupting the gel and leading to the rupture of the hydrogel microcapsules. Since the 5 wt-% alginate was able to provide the highest integrity of 90% in an excess amount of sulfate, it was selected for the preparation of the microcapsules in the subsequent tests. Note that the integrity needs to be further increased for applications under extreme conditions to prevent contamination in the Li^+ solution.

It is well documented that calcium also crosslinks with alginate [20], and it is readily accessible and low in price [17]. Calcium@alginate microcapsules prepared from the same method as the pure barium hydroxide Ba@alginate

microcapsules were able to achieve an integrity rate of 100%, higher than the Ba@alginate counterpart. This is because CaSO_4 is slightly soluble in water with a solubility constant K_{sp} of 1.9×10^{-4} , whereas BaSO_4 is insoluble with a K_{sp} of 6 orders smaller in magnitude [11]. Thus, Ca^{2+} is not as easily drained from the Ca@alginate gel in the presence of excessive sulfate. The greater stability of the calcium gel is also reflected in the use of CaSO_4 as a firming agent for alginate based gelation reactions in tissue engineering [21]. Therefore, calcium was selected as another crosslinking agent for the reinforcement of Ba@alginate in the two additional methods to produce Ca/Ba@alginate and Ca-Ba@alginate.

To prepare the Ca/Ba@alginate microcapsules, the concentration of the Ca^{2+} solution and the crosslinking time were optimised using the physical strength test. As shown in Fig. 3(b), microcapsules produced from $0.1 \text{ mol} \cdot \text{L}^{-1} \text{ Ca}^{2+}$ and 5 min gelation time was able to withstand 2 N of force before crushing, implying the microcapsules can stack within a packed column for approximately 1 m. For $0.05 \text{ mol} \cdot \text{L}^{-1} \text{ Ca}^{2+}$, it takes as long as 20 min to obtain a similar strength. The reaction was too fast to be controlled in solutions of Ca^{2+} concentrations higher than $0.1 \text{ mol} \cdot \text{L}^{-1}$. It is undesirable if the alginate inside a microcapsule is fully crosslinked by Ca^{2+} , as it loses the capacity for barium crosslinking.

3.3 Distribution of SO_4^{2-} adsorption sites on microcapsules

To investigate the distribution of the sulfate adsorbed by the Ba@alginate microcapsules, SEM/EDS was conducted to locate the key elements inside the microcapsules. The content of Ba and S in the Ba@alginate microcapsules before and after sulfate adsorption is presented in Figs. 4(a)–4(d), respectively. The SEM/EDS analyses require the sample to be completely dried, the microcapsules deformed after dehydration (Figs. 4(b) and 4(d)).

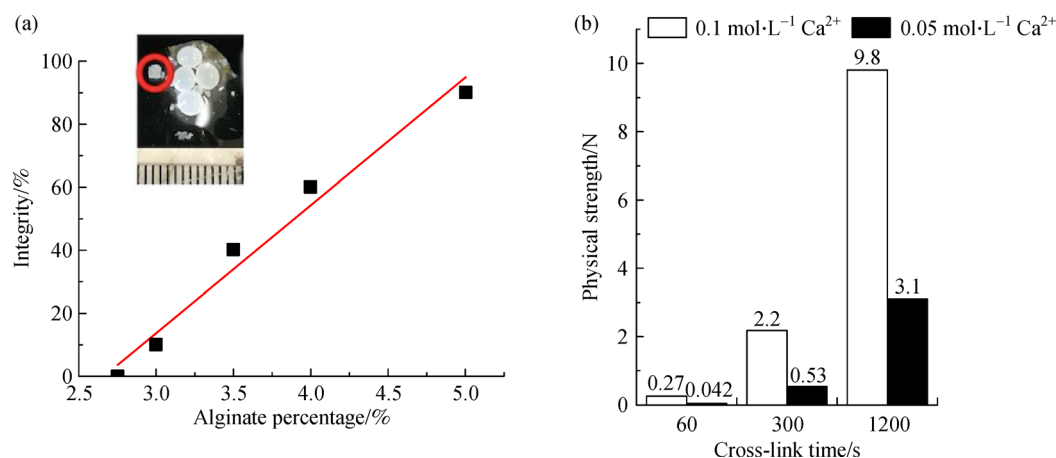


Fig. 3 (a) The relationship between the integrity and the concentration of alginate in an $800 \text{ mg} \cdot \text{L}^{-1}$ lithium sulfate solution (red line: a line of best fit; inset: optical image of Ba@alginate flakes, scale: mm); (b) the physical strength of calcium@alginate microcapsules under 0.1 and $0.05 \text{ mol} \cdot \text{L}^{-1} \text{ Ca}^{2+}$ and 60, 3000, 1200 s crosslink time.

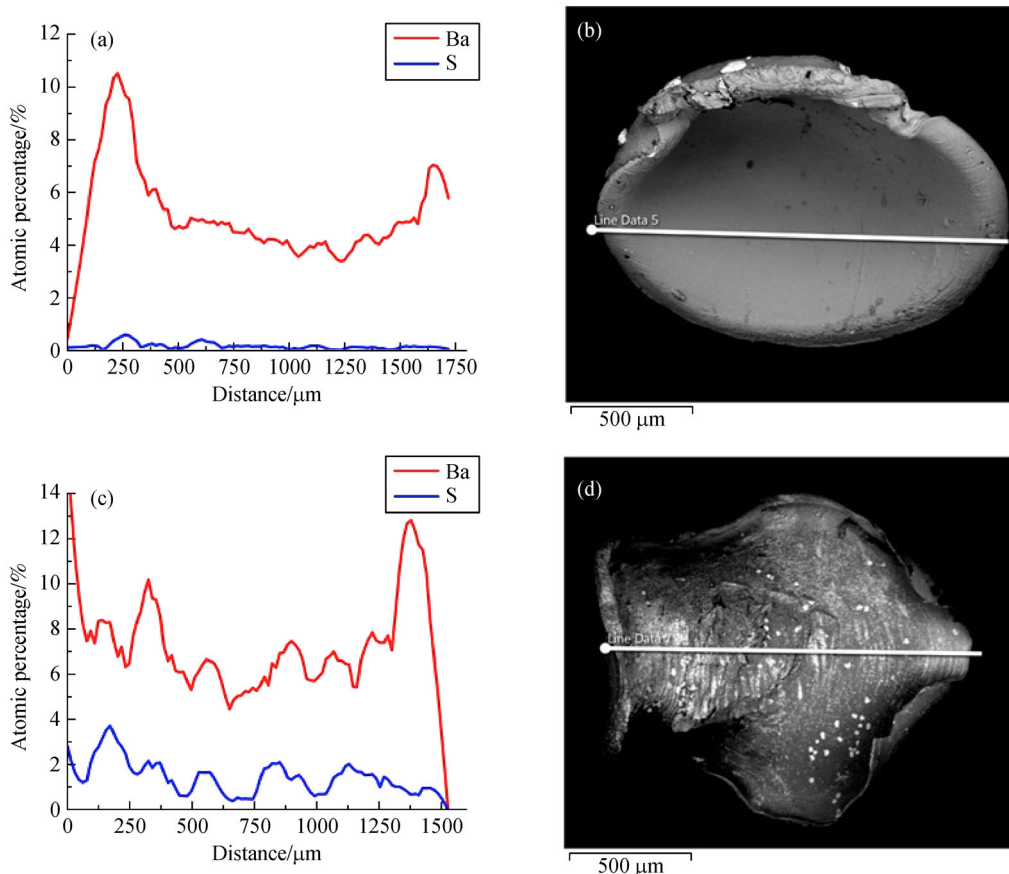


Fig. 4 SEM/EDS of pure barium hydroxide Ba@alginate microcapsules (a–b) before and (c–d) after sulfate adsorption in $100 \text{ mg} \cdot \text{L}^{-1}$ lithium sulfate solution. The distance on the x -axis corresponds to the chord line shown in the microscopy image.

The barium contents in both samples are similar, around 5%–10% along the chord of the cross-section under the EDS scan. However, the distribution of barium along the line is not even. This is very likely due to the geometric differences in height, when the Ba@alginate gel is closer to the electron receptor more signals were detected, resulting in a higher spectrum. Another reason could be the shrinking core reaction process [22] leading to higher barium in the outer layer than that in the core of the microcapsules. Before adsorption, the background sulfate concentration is very low, less than half an atomic percentage, as shown in Fig. 4(a). After adsorption, the sulfur content inside the microcapsule peaks at 3% (Fig. 4(c)), which is significantly higher than before. This observation clearly shows that the Ba@alginate microcapsules served as the sulfate adsorbent and successfully entrapped barium sulfate.

3.4 Effectiveness of sulfate removal

As discussed in section 3.3, the capsules contain 5%–10% barium, 0.2 g of microcapsules equal to 7.3×10^{-5} – 1.5×10^{-4} mol of barium which is well in excess of the 10 mL of

$100 \text{ mg} \cdot \text{L}^{-1}$ lithium sulfate present, which equals to 1.0×10^{-5} mol of sulfate ions. The efficiencies of sulfate removal and the resulting sulfate concentration achieved by Ba@alginate microcapsules are shown in Fig. 5.

The Ca/Ba@alginate microcapsules prepared by the two-step gelation method obtained the highest percentage of sulfate removal (99.9%), resulting in a sulfate concentration of $0.2 \text{ mg} \cdot \text{L}^{-1}$ in the lithium sulfate solution. This is significantly below the $20 \text{ mg} \cdot \text{L}^{-1}$ target. Furthermore, the Ca-Ba@alginate microcapsules achieved $9.4 \text{ mg} \cdot \text{L}^{-1}$ sulfate concentration for the treated solution after adsorption, which is still well below the $20 \text{ mg} \cdot \text{L}^{-1}$ allowable value. Finally, the Ba@alginate microcapsules achieved $16 \text{ mg} \cdot \text{L}^{-1}$ sulfate concentration after adsorption, which is sufficient for the target concentration, with 84% of the sulfate removed from the solution. During the production of battery grade lithium, sulfate is the major impurity that needs to be thoroughly removed. Other undesired species are very minor can include Cl^- , Mg^{2+} , Ca^{2+} , Fe^{3+} , K^+ , Na^+ [23]. However, they have no interference with the sulfate adsorption process and are normally removed by the re-crystallization process.

The addition of Ca^{2+} resulted in greater sulfate removal

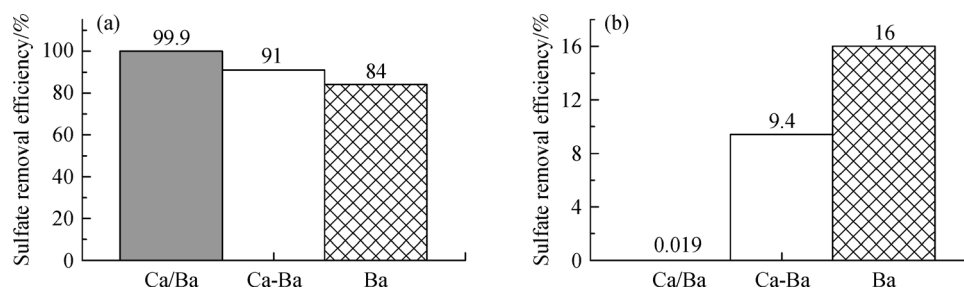


Fig. 5 (a) Sulfate removal efficiency of Ba@alginate microcapsules in a $100 \text{ mg} \cdot \text{L}^{-1}$ lithium sulfate solution; (b) concentration of sulfate solution after adsorption in a $100 \text{ mg} \cdot \text{L}^{-1}$ lithium sulfate solution.

effectiveness in both types of the reinforced microcapsules compared to the pure barium hydroxide Ba@alginate microcapsules. This is because the presence of barium in the gelling solution results in a lower permeability for the transfer of external ions through the microcapsules [24]. In this case, the Ba@alginate microcapsules were prepared from a pure barium hydroxide gelling bath, leading to the lowest permeability. Hence it is more difficult for the SO_4^{2-} ions to penetrate through the alginate gel and react with the Ba^{2+} ions.

On the other hand, the Ca/Ba@alginate microcapsules prepared by the two-step gelation method have the smallest amount of barium compared with other samples, as the calcium crosslinking reaction takes place before barium. In this method, intermediate Ca@alginate microcapsules were fabricated first, and a larger amount of calcium (compared with the Ca-Ba@alginate prepared by the dual-ion method) reacted with alginate to give the desired physical strength for the intermediate microcapsules. In contrast, for Ca-Ba@alginate microcapsules in which the Ca^{2+} and Ba^{2+} undergo gelation reaction at the same time, the Ba^{2+} ions have a higher affinity compared to Ca^{2+} , and thus a greater tendency to react with the free carboxyl functional groups. Therefore, the ion permeability of Ca/Ba@alginate is greater than the Ca-Ba@alginate, resulting in a higher sulfate removal efficiency. This result suggests that other multivalent cations can also be considered to reinforce the Ba@alginate microcapsules which can be explored in future work.

3.5 Kinetics analysis

The kinetics of the sulfate removal process for the Ba@alginate microcapsules are shown in Fig. 6. It can be seen that the initial adsorption of sulfate Q increases quickly during the first 30 min, reaching 85% of the maximum capacity, then the adsorption reactions slow down and plateau to an equilibrium value at about 1 h. With the maximum capacity of over $1.5 \text{ mg} \cdot \text{g}^{-1}$, the Ba@alginate microcapsules showed a much better adsorption performance than other potential adsorbents, such as the polystyrene divinylbenzene (PS-DVB) copolymer beads with the sulfate adsorption capacity of $0.318 \text{ mg} \cdot \text{g}^{-1}$

[25], which is about 5 times lower. In optimum condition, the sulfate removal efficiency from saline water of PS-DVB was 65.64%, whereas our Ba@alginate microcapsules show removal efficiency of 84%, and our other adsorbent Ca/Ba@alginate microcapsules show removal efficiency of over 99% (Fig. 5(a)). The amount of sulfate removed by the Ba@alginate microcapsules decreases from the initial maximum capacity of $2 \text{ mg} \cdot \text{g}^{-1}$ to a new equilibrium value of $1.5 \text{ mg} \cdot \text{g}^{-1}$ after 1 h of adsorption. This unexpected result may be because a small fraction of the sulfate that was physically adsorbed initially in the microcapsules was released back to the solution as the Ba@alginate gel de-crosslinked due to the competitive adsorption of sulfate. The data points after the 1 h mark for the Ba@alginate microcapsules were not included in the fitting of kinetic models.

The time dependent removal rate of sulfate per gram of microcapsules over time in Fig. 6 was fitted with the pseudo second order (Fig. 6(a)), pseudo first order (Fig. 6(b)), and Elovich models (Fig. 6(c)) [26] using Eqs. (4), (5) and (6), respectively:

$$Q = k_2 Q_e^2 \frac{t}{1 + k_2 Q_e t}, \quad (4)$$

$$Q = Q_e (1 - \exp(-k_1 t)), \quad (5)$$

$$Q = \frac{1}{\beta} \ln(1 + \alpha \beta t), \quad (6)$$

where k_1 (s^{-1}) and k_2 ($\text{g} \cdot \text{mg}^{-1} \cdot \text{s}^{-1}$) are adsorption rates for pseudo first and second order, respectively; Q is the amount of sulfate removed at time t (s); Q_e ($\text{mg} \cdot \text{g}^{-1}$) is the maximum amount of sulfate adsorbed by the microcapsules at equilibrium. For the Elovich model, the adsorption rate is described by $k_E = \alpha \exp(-\beta Q)$.

Among the three models, the pseudo second order model gives the best fit with the experimental data for all three types of microcapsules. As summarised in Table 1, the correlation coefficient, R^2 , is 0.990, 0.991, and 0.984 for Ba@alginate, Ca/Ba@alginate, and Ca-Ba@alginate microcapsules, respectively. For the pseudo second order model, the maximum capacity of sulfate at equilibrium for

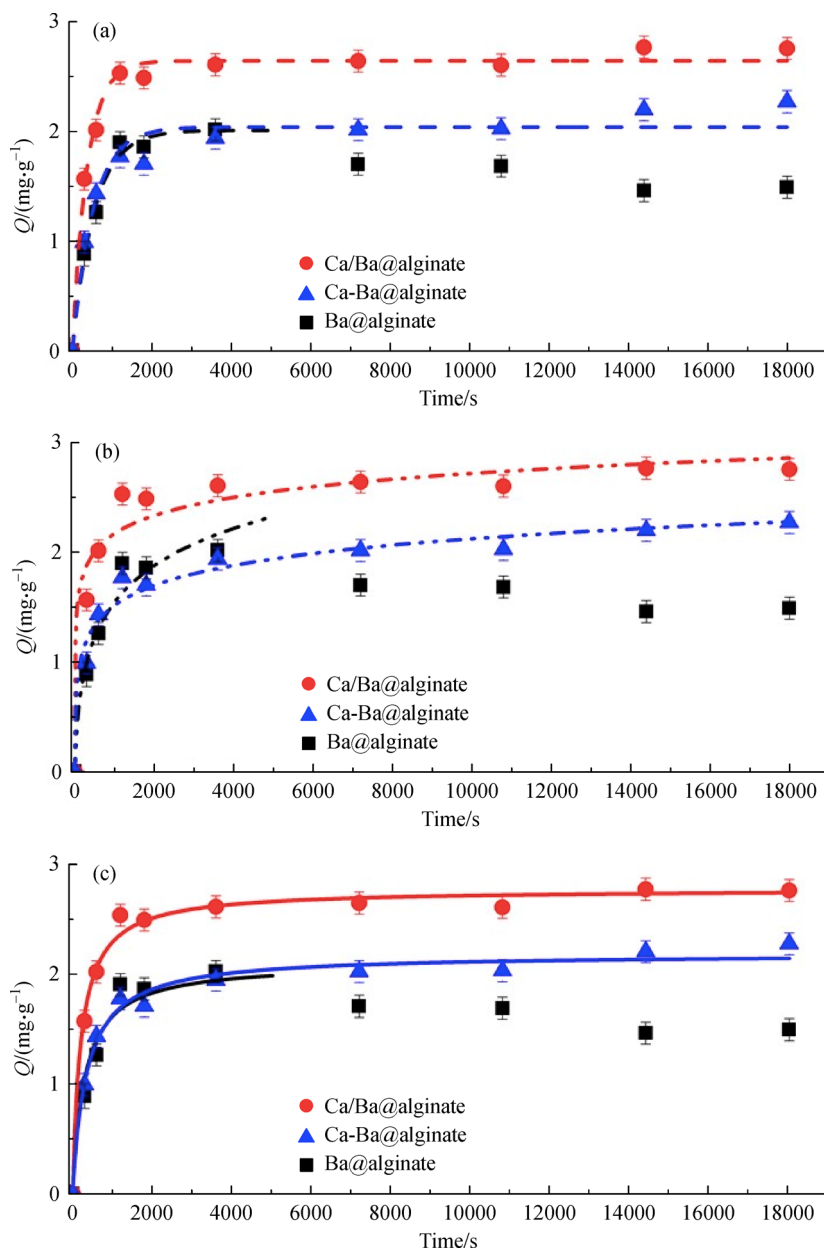


Fig. 6 The sulfate removed per gram of Ba@alginate microcapsules in $100 \text{ mg} \cdot \text{L}^{-1}$ lithium sulfate solution versus time fitted by (a) the pseudo second order, (b) pseudo first order, and (c) Elovich adsorption kinetic models.

the two-step Ca/Ba@alginate is the highest at $2.76 \text{ mg} \cdot \text{g}^{-1}$. The equilibrium adsorption capacity of sulfate for pure barium hydroxide Ba@alginate and the one step dual-ion Ca-Ba@alginate microcapsules are similar at $2.10 \text{ mg} \cdot \text{g}^{-1}$ and $2.18 \text{ mg} \cdot \text{g}^{-1}$, accordingly, with Ca-Ba@alginate slightly higher. The adsorption rate (k_2) for the two-step Ca/Ba@alginate microcapsules is $1.71 \times 10^{-3} \text{ g} \cdot \text{mg}^{-1} \cdot \text{s}^{-1}$ being the highest of the three types which implies that the Ca/Ba@alginate microcapsule adsorb sulfate in a solution fastest.

The results of these adsorption kinetics experiments are consistent with the sulfate removal efficiency test where the

two-step Ca/Ba@alginate microcapsules also gave the best sulfate adsorption capacity. On the other hand, the Ba@alginate and Ca-Ba@alginate microcapsules have k_2 coefficients of $1.56 \times 10^{-3} \text{ g} \cdot \text{mg}^{-1} \cdot \text{s}^{-1}$ and $1.32 \times 10^{-3} \text{ g} \cdot \text{mg}^{-1} \cdot \text{s}^{-1}$, respectively. This means that the Ba@alginate microcapsules adsorb sulfate faster than the Ca-Ba@alginate microcapsules, although the permeability in the Ca-Ba@alginate microcapsules is slightly higher than that in the Ba@alginate microcapsules, as discussed before (Section 3.4). This is because the adsorption reaction is governed by both the permeability of the sulfate ions through the microcapsules as well as the adsorption site

Table 1 Kinetic parameters of second order pseudo, first order pseudo, and Elovich for Ba@alginate microcapsules in 100 mg·L⁻¹ lithium sulfate solution

Parameters	Secondorder pseudo			Firstorder pseudo			Elovich		
	Q_c /(mg·g ⁻¹)	$k_2 \times 10^{-3}$ /(g·mg ⁻¹ ·s ⁻¹)	R^2	Q_c /(mg·g ⁻¹)	$k_1 \times 10^{-3}$ /s ⁻¹	R^2	α /s ⁻¹	β	R^2
Ca/Ba@alginate	2.76	1.71	0.991	2.64	2.68	0.988	2.08	4.19	0.952
Ca-Ba@alginate	2.18	1.32	0.984	2.04	1.91	0.953	8.25×10^{-3}	3.80	0.971
Ba@alginate	2.10	1.56	0.990	2.01	1.83	0.990	1.07×10^{-2}	2.02	0.955

available in the outer layers. The Ba@alginate microcapsules have a higher barium content compared to the Ca-Ba@alginate microcapsules, and hence the rate of adsorption is faster at the beginning. However, due to the limitation of the sulfate permeability through the microcapsules the adsorption capacity of the Ca-Ba@alginate microcapsules plateaus at a higher equilibrium value. The other two models with slightly lower R^2 values also suggest that the two-step Ca/Ba@alginate microcapsules are the best among the three samples.

4 Conclusions

We have prepared Ba@alginate microcapsules as a novel adsorbent for lithium purification in lithium refining to remove sulfate in solution. Three methods were developed namely pure barium hydroxide Ba@alginate, two-step Ca/Ba@alginate, and the one step dual-ion Ca-Ba@alginate for preparing three varieties of microcapsules. The Ba@alginate microcapsules could successfully remove sulfate from the lithium sulfate solution, reducing its concentration to 16 mg·L⁻¹. Although the addition of calcium did not further improve the integrity of the microcapsules, it increased the effectiveness of sulfate removal. The two-step Ca/Ba@alginate microcapsules showed the highest rate of adsorption and the greatest sulfate removal rate, achieving a sulfate concentration (as low as 0.02 mg·L⁻¹) that is three orders of magnitude below the impurity limit of sulfate for producing battery-grade lithium. Furthermore, the Ba@alginate microcapsules have the advantages of ease of preparation, high efficiency, low cost, and adaptability to commercialise adsorption technologies, demonstrating great potential for future applications in lithium refining processes.

Acknowledgements This work was supported by the Department of Chemical Engineering at The University of Melbourne.

References

1. Hykawy J, Chudnovsky T. Industry report//Lithium. Stormcrow technical report. 2015
2. Grosjean C, Miranda P H, Perrin M, Poggi P. Assessment of world

- lithium resources and consequences of their geographic distribution on the expected development of the electric vehicle industry. *Renewable & Sustainable Energy Reviews*, 2012, 16(3): 1735–1744
3. Kesler S E, Gruber P W, Medina P A, Keoleian G A, Everson M P, Wallington T J. Global lithium resources: relative importance of pegmatite, brine and other deposits. *Ore Geology Reviews*, 2012, 48: 55–69
4. Chen Y, Tian Q, Chen B, Shi X, Liao T. Preparation of lithium carbonate from spodumene by a sodium carbonate autoclave process. *Hydrometallurgy*, 2011, 109(2): 43–46
5. Peiró L T, Méndez G V, Ayres R U. Lithium: sources, production, uses, and recovery outlook. *JOM*, 2013, 65(8): 986–996
6. Buckley D, Genders J D. Method of making high purity lithium hydroxide and hydrochloric acid. US Patent, 20110044882A1, 2011-02-24
7. Livent. Lithium hydroxide monohydrate, battery grade. Datasheet. 2018
8. Wang L K, Vaccari D A, Li Y, Shammam N K. Physicochemical Treatment Processes. In: *Handbook of Environmental Engineering*. New Delhi: Humana Press, 2005, 3: 141–197
9. Sarkar S, Sengupta A K, Prakash P. The Donnan membrane principle: opportunities for sustainable engineered processes and materials. *Environmental Science & Technology*, 2010, 44(4): 1161–1166
10. Tang C Y, Yang Z. Transmission electron microscopy (TEM). *Membrane Characterization*, 2017, 145–159
11. Lin S. *Water and wastewater calculations manual* 3rd edition, 2014
12. Chen G G, Luo G S, Xu J H, Wang J D. Membrane dispersion precipitation method to prepare nanoparticles—A Review. *Powder Technology*, 2004, 139(2): 180–185
13. Wong D C Y, Jaworski Z, Nienow A W. Effect of ion excess on particle size and morphology during barium sulfate precipitation: an experimental study. *Chemical Engineering Science*, 2001, 56(3): 727–734
14. Lee K Y, Mooney D J. Alginate: properties and biomedical applications. *Progress in Polymer Science*, 2012, 37(1): 106–126
15. Lu D R, Xiao C M, Xu S J. Starch-based completely biodegradable polymer materials. *Express Polymer Letters*, 2009, 3(6): 366–375
16. Li Z, Ramay H R, Hach K D, Xiao D, Zhang M. Chitosan-alginate hybrid scaffolds for bone tissue engineering. *Biomaterials*, 2005, 26(18): 3919–3928
17. Fiol N, Escudero C, Poch J, Villaescus I. Preliminary studies on Cr (VI) removal from aqueous solution using grape stalk wastes encapsulated in calcium alginate beads in a packed bed up-flow column. *Reactive & Functional Polymers*, 2006, 66(8): 795–807

18. Lee B B, Ravindra P, Chan E S. Size and shape of calcium alginate beads produced by extrusion dripping. *Chemical Engineering & Technology*, 2013, 36(10): 1627–1642
19. Chan E S, Lee B B, Ravindra P, Poncelet D. Prediction models for shape and size of ca-alginate macrobeads produced through extrusion-dripping method. *Journal of Colloid and Interface Science*, 2009, 338(1): 63–72
20. Papageorgiou S K, Kouvelos E P, Katsaros F K. Calcium alginate beads from *Laminaria digitata* for the removal of Cu^{2+} and Cd^{2+} from dilute aqueous metal solutions. *Desalination*, 2008, 224(1-3): 293–306
21. Larsen B E, Bjørnstad J, Pettersen E O, Tønnesen H H, Melvik J E. Rheological characterization of an injectable alginate gel system. *BMC Biotechnology*, 2015, 15(1): 29
22. Fogler H S. *Elements of Chemical Reaction Engineering*. 5th ed. New Jersey: Prentice Hall, 2016, chapter 14: 1–10
23. Cai W, Chen R, Yang Y, Yi M, Xiang L. Removal of SO_4^{2-} from Li_2CO_3 by recrystallization in Na_2CO_3 solution. *Crystals*, 2018, 8(1): 19–26
24. Mørch Ý A, Donati I, Strand B L, Skjåk-Bræk G. Effect of Ca^{2+} , Ba^{2+} , and Sr^{2+} on alginate microbeads. *Biomacromolecules*, 2006, 7(5): 1471–1480
25. Fathy M, Moghny T A, Awadallah A E, Au El-Bellihi A. Study the adsorption of sulfates by high cross-linked polystyrene divinylbenzene anion-exchange resin. *Applied Water Science*, 2017, 7(1): 309–313
26. Largitte L, Pasquier R. A review of the kinetics adsorption models and their application to the adsorption of lead by an activated carbon. *Chemical Engineering Research & Design*, 2016, 109: 495–504